Bremsstrahlung analysis through the microwave cutoff, and afterglow performances

M. Lamoureux
Laboratoire de Dynamique des Ions, Atomes et Molecules, C75, Université P. et M. Curie, 4 place Jussieu, 75252, Paris, France

V. Mironov
Laboratory of Particle Physics, Joint Institute for Nuclear Research, Dubna, 141980, Russia

M. Niimura, M. Kidera, T. Nakagawa
The Institute of Physical and Chemical Research (RIKEN), Hirosawa 2-1, Wako, Saitama 351-0198, Japan

The enhancement of high charge state currents provided by the afterglow effect is investigated in its relation with the intensity of the hard X-ray emission. The best operating conditions were found to be different, depending on whether the ECRIS is operated in the continuous or afterglow mode. Bigger afterglow peak currents can be obtained when a more intense X-ray emission has been observed before the rf power is shut off (though the currents themselves may be the same at that time .....). The perpendicular temperature parameter T_{perp} and the density $N_{e,hot}$ relative to the hot electron population responsible for that emission are estimated as a function of time. The results support the view that the afterglow effect is due to a fast modulation of the ECRIS plasma potential. A couple of experimental estimates are also given for the maximum energy E_{max} reached by the hot electrons in the continuous mode.

I. Introduction

Bremsstrahlung spectra with a good energy resolution have been obtained at the RIKEN 18 Ghz ECRIS, throughout the radio-frequency (rf) switch off, for various time slabs from 3 to 10 msec. The experimental set-up and the detection chain have been described in details elsewhere [1] together with some discussions on the main conclusion: the largest afterglow currents of highly charged ions appear to be obtained when intense X-rays are observed in the heating or steady-state stage. This is qualitatively coherent with

a recent remark, made in passing, by Hill and Langbein [2] who are exploiting at CERN the afterglow effect whose interest had been demonstrated at CERN some years earlier [3]. The authors of ref.[2] state indeed that " certain operating points gave rise to increased X-ray emission ".

Fig.1 immediately illustrates this result involving the afterglow current peak and the X-ray emission. It plots the number of high energy photon counts detected, for a strong (upper curve) and a mediocre (lower curve) afterglow effect.

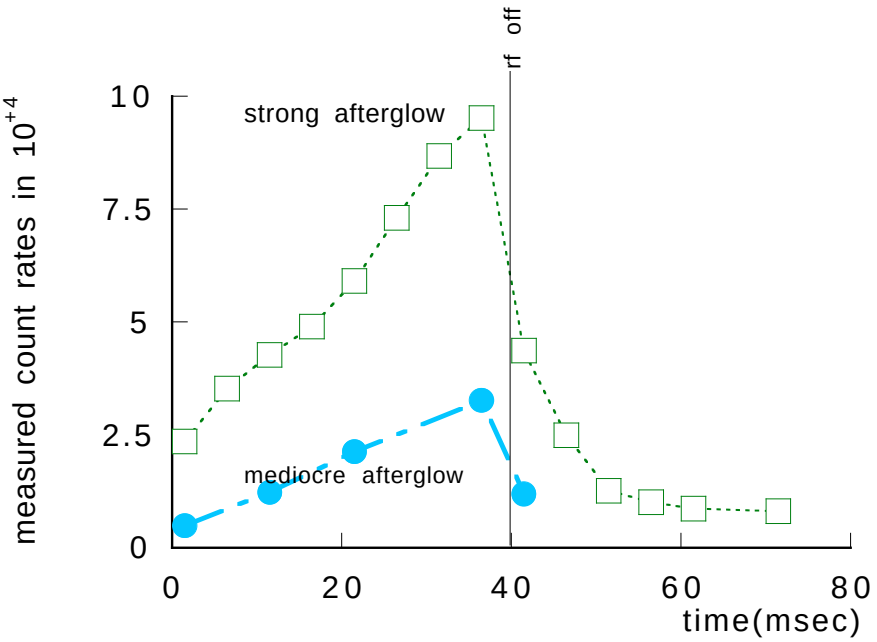

Fig.1. Total photon count rate registered by the detector for energies above 150 keV. Comparison between a strong and a mediocre afterglow enhancement of the Ar^{9+} current. The repetition rate is 9 Hz. The time slab is 3 msec. The rf power of 50W is applied at t=0 and turned off at t=40 msec. Data taken from ref.[1].

The operating conditions were identical in these two cases except for the value of the B_{max} magnetic field on the extraction side. In both cases, the Ar^{9+} current was the same right before the rf was turned off, i. e. at t=40 msec, but it gets amplified differently at the rf turn-off. In the first case, the ratio of the peak afterglow current to the current found right before the rf was turned off is in the ratio 1.3/1. In the second case corresponding to a larger B_{max} , this amplification is increased to 3/1. This comparison lead to the schematic remark: a bigger B_{max} on the extraction side jointly leads to a stronger X-ray emission (signaling a richer hot electron component) and to a larger afterglow enhancement. These results already shown in ref.[1] receive below some qualitative comments by the analysis of new series of bremsstrahlung spectra.

II. Analysis of the bremsstrahlung spectra throughout the rf cutoff: evolution of the temperature and density of the hot electrons.

Attempts are made to characterize the hot electron population versus time, including beyond the rf turn-off moment, whereas that characterization had been done [4] so far only in relation with the oscillatory regime that appears in the continuous mode either at too high powers or at too low pressures. The study is made for the better afterglow case. A Cu collimator was located in front of the detector, as well as a thin 0.8 mm Cu plate; the detector itself was shielded by a Pb cover. Spectra are given in Fig.2a and Fig.3a for the heating and cooling stages respectively. The repetition rate is now 2 Hz, and the rf power of 50 W is cut off at t=100 msec. The gas pressure is $2x10^{-7}$ Torr for the optimized Ar^{9+} current. The gate duration is 10 msec, and the time slabs considered are indicated on the curves. The data are accumulated over 2000 pulses.

a) spectrum

b) noise spectrum

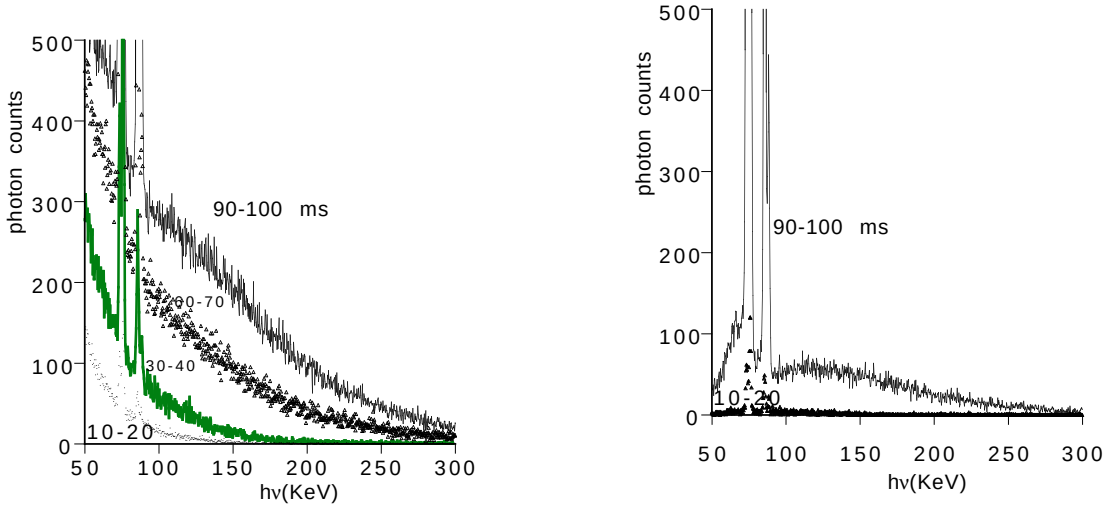

Fig.2 Bremsstrahlung spectra obtained in the heating stage for various time slabs. The rf power is applied at t=0.

a) spectrum

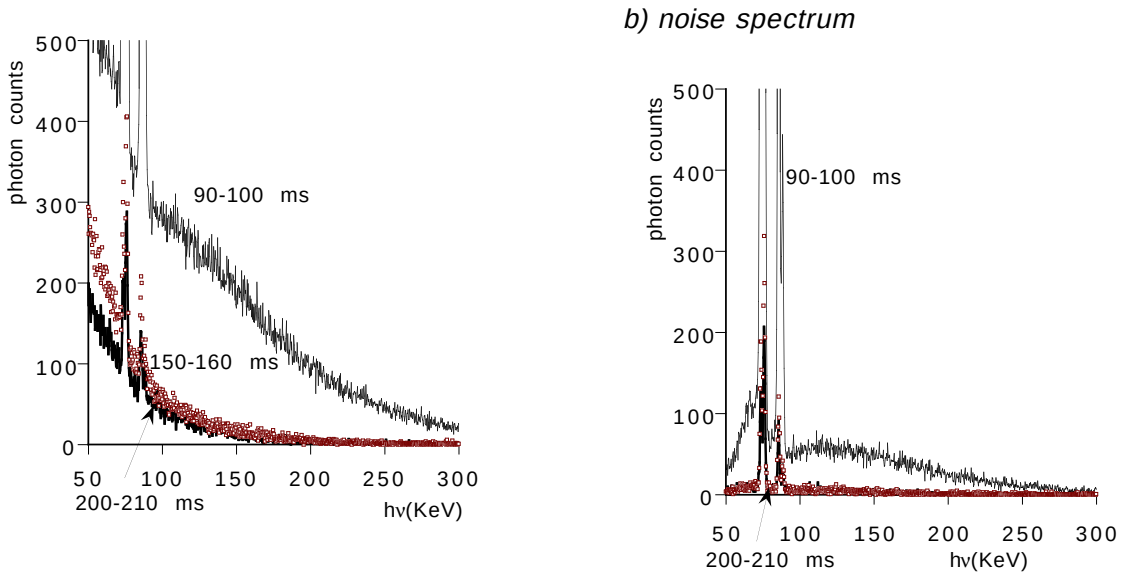

Fig.3 Bremsstrahlung spectra obtained in the cooling stage for various time slabs. The rf power of 50 W has been turned off at t=100 msec.

Since the collimating system is not as elaborate as in ref.[4], the present data could not be treated as such, and some non negligible background noise was recorded in a second series of experiments by using a supplementary 10 mm thick Pb plate in front of the detector (See Fig.2b and Fig.3b). The Pb discontinuities in the spectra, especially for the second series of experiments, prevents any analysis below 110 keV or so. Above that energy, the photons attributed to the ECRIS bremsstrahlung are evaluated by the formula

$$N(h\nu) = \frac{N_{0.8Cu,10Pb}(h\nu) - N_{10Pb}(h\nu)}{\alpha_{0.8\mathrm{Cu}}(h\nu)\left[1-\alpha_{10Pb}(h\nu)\right]} \approx \frac{N_{0.8Cu,10Pb}(h\nu) - N_{10Pb}(h\nu)}{\alpha_{0.8\mathrm{Cu}}(h\nu)}$$

where the indices, for the count numbers N and for the absorption coefficients α, refer to the presence of one or two plates in front of the detector. The hot electron temperature was then obtained as explained in ref. [5], but after having adapted the diagnostic to the present atomic number and to the exploitable photon regions suggested by the spectra. For example, the energy domains 100-150 keV, 150-180 and then 150-300 keV were choosen for the various time slabs, in order to ensure enough precision and also enough security against the pile-up danger that is likely to happen at the most radiative moments. Let us recall that the diagnostic assumes that the hot electrons are moving in a plane perpendicular to the main magnetic axis and are following a non-Maxwellian distribution roughly of the shape $E\exp\left(-E/kT_{perp}\right)$. Because of these assumptions and of the not excellent precision of the present experimental data, the values given in Fig.4 cannot be taken at face value, and only the trends are reliable. The values of T_{perp} are obtained by fitting the shape of the calculated spectrum to the shape of the observed one, and the hot electron density $N_{e,hot}$ is then given by the ratio of the measured emissivity to the one calculated at that T_{perp} for the center of the photon energy domain considered.

Fig.4 indicates that the hot electron temperature parameter T_{perp} saturates earlier than the hot electron density $N_{e,hot}$.

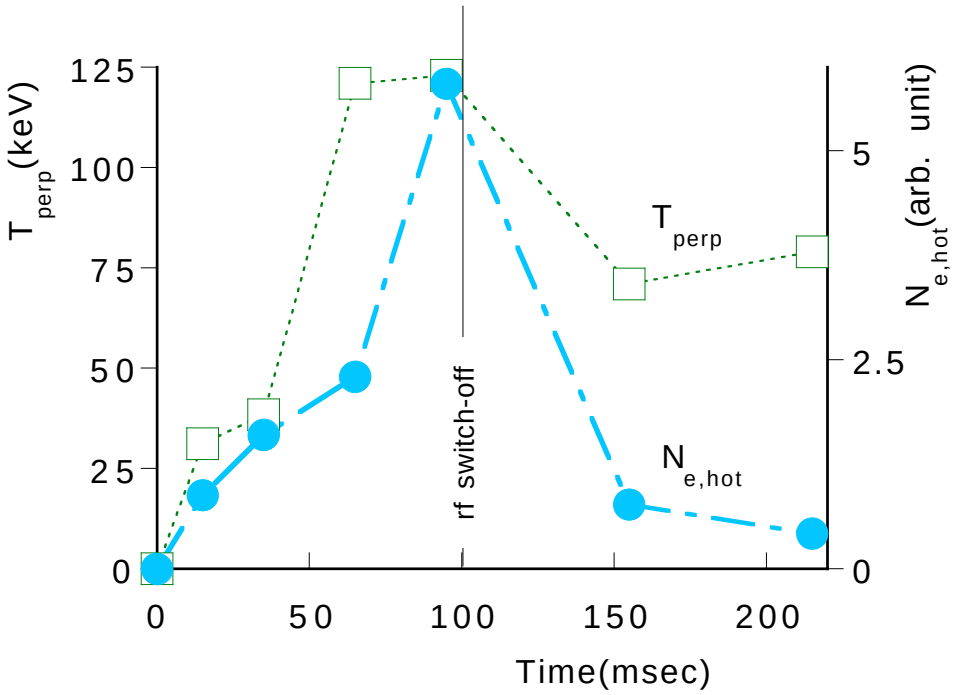

Fig. 4. Estimates of the perpendicular temperature and of the hot electron density deduced from the spectra of figs.2-3. (Lines are drawn only to guide the eye). The rf is applied at t=0 and turned off at t=100 msec.

Beyond t=50 msec, only the density goes on increasing. Right after the rf is turned off, T_{perp} drops more moderately than $N_{e,hot}$. After this drop, both quantities remain nearly constant. This evolution with time after the rf turn-on is to be paralleled with a few results obtained with Quadrumafios [6] in Grenoble at steady state, where T_{perp} and $N_{e,hot}$ are given for various powers. At a fixed gas injection pressure, T_{perp} increases much less than $N_{e,hot}$ with higher powers. The survival of high energy photons and thus of energetic electrons was also observed in Quadrumafios[4b]. In the present case, we could observe some high energy photons even 400 msec after the rf turn-off.

III. Estimates of the maximum electron energy

In order to trace back the high energy range and the maximum energy reached by the electrons, the observation conditions had to be changed because the emission was already very small at 300 keV (See Figs. 2-3). In order to favor the detection of the high energy photons, the collimator was removed, and the thin Cu plate in front of the detector was replaced by a 2 mm thick Pb plate.

a)

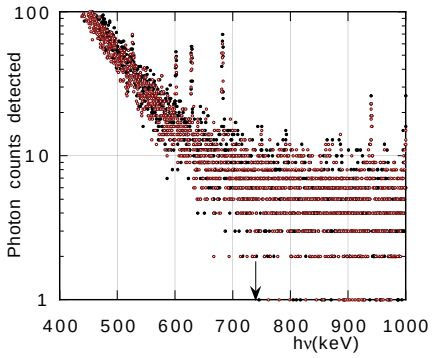

b)

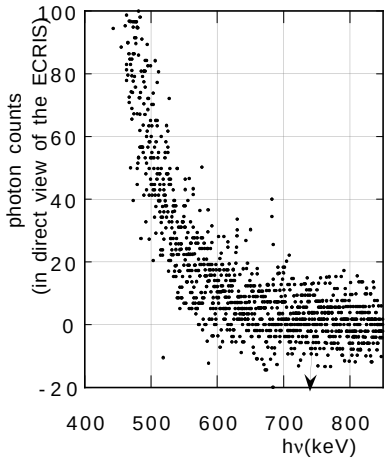

Fig.5. High energy spectra.
Fig.5a, directly recorded spectrum.
Fig.5b, spectrum obtained after having taken into account the background noise.
Observation of the maximum energy reached by the photons (and hence by the electrons) in the continuous mode. For the rf power of 50 W, E_{max} is about 740 keV.

Fig. 5a shows the end spectrum obtained in the direct measurements for the rf power of 50 W, and Fig.5b shows the number of photons emitted by the ECRIS region of interest, calculated as above by taking into account the background noise. The change of behavior in Fig.5a occurs at 740 keV with an uncertainty perhaps as high as 25 keV, and the asymptotic value zero is reached also at 740±25 keV in Fig.5b. This value can thus be assimilated to the maximum energy E_{max} reached by the electrons. Two similar experiments were done for the power of 100 W, and the maximum energy observed was about 940 keV. Though we have only two approximate values of E_{max}, it is worthwhile mentioning that their ratio 940/740=1.27 is very close to $(100/50)^{3/8}$ = 1.30, as expected from the power laws indicated in Geller's book [7]. This brings some confirmation on how the electrons are heated in the plasma, but little remains known on the dynamics of the electrons in the cooling stage.

IV Conclusion

Concluding now on the afterglow mode, some hand-waving reasoning can explain why the best operating conditions are not the same in the continuous mode and in the afterglow mode. The current output in the former case is known to be a compromise between an efficient production of high charge ions inside the plasma and an easy extraction. To that respect, the building up of a large electron component has two opposite effects because it goes together with a better confinement. This competition is

best seen in calculations based on the scenario involving a potential dip in the calculations of the ionic populations and currents[8]. In the continuous mode, this component should not be increased beyond some point for fear of deteriorating the extraction. In our case for example, the output current in Ar^{9+} and the temperature T_{perp} already saturates at t=50 msec, wheareas the hot electron density is at that moment only about a third of its value at t=100 msec (See Fig.4). At times later than 50 msec, a larger ionic population can be produced; moreover the bigger electron population will produce a stronger change of the plasma potential, which favors the expulsion of these ions when the rf is turned off. For similar reasons, a larger B_{max} fied on the extraction side also favors the electron confinement and increases the electron density. The resulting afterglow current, together with the X-ray emission right before the rf turn-off, are therefore jointly enlarged.

Acknowledgements.
Two of us (M. L. and V. M.) acknowledge the Institue of Physical and Chemical Research (RIKEN) for a stay at the Cyclotron Laboratory in spring 1998.

[1] M. Kidera, M. Lamoureux, V. Mironov, T. Nakagawa and G. Shirkov, accepted for publication at Rev. Sci. Instrum. (revised version recently submitted).
[2] C. E. Hill and K. Langbein, Proceedings of the 7 th International Conference on Ion Sources, Taormina, Italy, 7-13 Sept . 1997. Rev. Sci. Instrum, **69**, 643 (1998).
[3] P. Briand, G. Geller and G. Melin, Nucl. Instrum. Methods, **A294**, 673 (1990).
[4] M. Lamoureux, A. Girard, R. Pras, P. Charles, H. Khodja, F. Bourg, J. P. Briand, and G. Melin, Physics of Plasmas, **2**, 12 (1996), also 4b: same authors, proceedings of 13 th International workshop on ECR on Ion Sources (College Station, USA, February, 1997) p 67.
[5] C. Barué, M. Lamoureux, P. Briand, A. Girard and G. Melin, J. App. Phys. **76**, 2662 (1994); also 5b: M. Lamoureux, proceedings at 12 th International workshop on ECR Ion Sources, (Riken, April 1995) p 74.
[6] R. Pras, thèse de l'Université de Pierre et Marie Curie, Paris (1997), in French.
[7] R. Geller, *Electron Cyclotron Resonance Ion Sources and ECR Plasmas* (Institute of Physics, Publishing Bristol and Philadelphia, 1996), p 194.
[8] R. Pras, M. Lamoureux, A. Girard, H. Khodja , and G. Melin, Proceedings of the 7 th International Conference on Ion Sources, Taormina, Italy, 7-13 Sept . 1997. Rev. Sci. Instrum. **69**, 700 (1998).